

Supporting Information

High-Entropy Oxide Hollow Spheres as Efficient Catalysts to Accelerate Sulfur Conversion Kinetics toward Lithium-Sulfur Batteries

Shuang Yu,^{‡a} Yingying Song,^{‡a} Xueda Li,^a Fang Liu,^a Huining Chang,^a Hongqiang Wang,^{*a} Jiao Li^{*a}

^aSchool of Materials Science and Engineering, Shandong University of Technology, Zibo, Shandong, 255000, P. R. China

[‡] These authors have contributed equally to this work.

* Corresponding authors.

E-mail: hwang@sdut.edu.cn (H. Wang)

haiyan9943@163.com (J. Li)

1. Experimental section

1.1 Calculation of configuration entropy

Because the anion position is only occupied by oxygen in transition metal (TM) oxides, a variety of TM cations have a great influence on the configuration entropy (S_{config}) of TM oxides. As such, the S_{config} of HEO with N-species components can be calculated by the following equation:

$$S_{config} = -R \sum_{i=1}^N \{x_i \ln(x_i)\} \quad (1-1)$$

cation-site

where x_i refers to the mole fraction of the cationic components, and R is the molar gas constant. Based on the above equation, the mixed S_{config} of any polymetallic oxide can be obtained. Using the S_{config} of 1 R and 1.5 R as the dividing line, the metal oxide can be divided into HEO, medium entropy oxide (MEO), and low entropy oxide. Therefore, the HEO system composed of 5 species in our paper has the S_{config} of 1.61 R, while the MEO system composed of 3 species has the S_{config} of 1.10 R.

1.2 Preparation of carbon spheres

Briefly, 0.5 mol L⁻¹ glucose solution (40 mL) was sealed into a 50 mL Teflon reactor with 180 °C for 6 h. The resulting products were washed and centrifuged with DI water, then dried under vacuum at 60 °C overnight.

1.3 Synthesis of HEO hollow spheres and HEO@S composite

250 mg of freshly prepared carbon spheres were first dispersed in 20 mL of DI water. Then, 0.009 mol of Fe(NO₃)₃·9H₂O, Co(NO₃)₂·6H₂O, Ni(NO₃)₂·6H₂O, Cu(NO₃)₂·6H₂O, and Zn(NO₃)₂·6H₂O with equimolar ratio were added to the above

suspension and stirred at room temperature for 12 h to obtain the HEO-carbon sphere (HEO-CSs) precursor. Subsequently, HEO-CSs precursors were dried overnight at 60 °C after suction filtration. Finally, HEO-CSs precursors were calcined at 500 °C for 2 h in air to obtain HEO hollow spheres. The HEO hollow spheres and sulfur were mixed with a mass ratio of 30:70 to obtain HEO@S composite by melting method.

1.4 Preparation of MEO, MEO@S, and C@S composite

Medium-entropy oxide (MEO) hollow spheres were prepared by the same procedure of HEO, but only using $\text{Fe}(\text{NO}_3)_3 \cdot 9\text{H}_2\text{O}$, $\text{Co}(\text{NO}_3)_2 \cdot 6\text{H}_2\text{O}$, and $\text{Ni}(\text{NO}_3)_2 \cdot 6\text{H}_2\text{O}$ as metal sources. The MEO hollow spheres were mixed with sulfur in a mass ratio of 30:70 to obtain MEO@S composite by melting method. C@S composite is prepared by using carbon black and sulfur with the same content via same procedure.

1.5 Characterization

The crystal structure was analyzed using X-ray diffraction with Cu-K_α radiation (BRUKER, D8 ADVANCE). The microstructure and elemental composition of the electrodes were characterized by field emission scanning electron microscopy (FEI, Nova Nano SEM 450) and transmission electron microscopy (FEI, Tecnai G2 F30). X-ray photoelectron spectroscopy (XPS) measurements were conducted using a K-Alpha spectrometer from Thermo Scientific, with an Al K_α excitation source. Ultraviolet-visible absorption experiments were performed using a UV-2600 spectrophotometer (Tian Mei).

1.6 Electrochemical measurements

1.6.1 Preparation of sulfur cathodes and electrochemical test

The sulfur electrode slurry was obtained by mixing active material, polyvinylidene fluoride (PVDF), and carbon black (8:1:1 by weight) in N-methyl-2-pyrrolidinone, which was coated on aluminum foil and then dried at 60 °C for 24 h. The CR2032 coin cells were assembled in an argon-filled glove box, using lithium foil as the anode and Celgard 2400 as the separator. The electrolyte consists of 1 M lithium bis (trifluoromethanesulfonyl) imide (LiTFSI) mixed with 1,3-dioxolane (DOL) and 1,2-dimethoxyethane (DME) in a volume ratio of 1:1, containing 1 wt% LiNO₃. The electrochemical performance of sulfur electrodes was evaluated in the voltage range from 1.8 to 2.6 V using a LAND CT2001A battery testing system. Additional electrochemical tests, such as cyclic voltammetry (CV) and electrochemical impedance spectroscopy (EIS), were performed on a CHI 660e electrochemical workstation.

1.6.2 Symmetrical batteries test

Two identical electrodes (HEO, MEO, and C) were placed on either side of the coin cell, and 30 μL Li₂S₆ electrolyte was added. CV measurements of symmetrical cells were taken at a voltage range of -1 to 1 V using the CHI 660e electrochemical workstation, and EIS measurements were conducted in frequency range of 0.01 Hz to 100 kHz.

1.6.3 Li₂S₆ Adsorption test

Firstly, Li₂S₆ solution was prepared. The sulfur powder and lithium sulfide (Li₂S) with a molar ratio of 5:1 were added into a mixture of 1,2-dimethoxyethane (DME) and 1,3-dioxolane (DOL) with volume ratio of 1:1 and heated at 60 °C in an Ar-filled glove box for 24 h. Subsequently, 15 mg HEO hollow spheres, MEO hollow spheres, and C

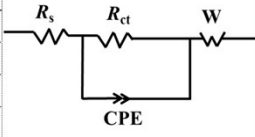
material were added to 2 mL Li_2S_6 solution for 6 h, respectively. The supernatant after adsorption was removed with a straw for UV-visible spectra test, and the powder samples were collected for XPS measurements.

1.6.4 Li_2S nucleation test

Li_2S and S (molar ratio of 1:7) were dissolved in a mixture of DOL and DME (volume ratio of 1:1), and vigorously stirred at 60 °C for 24 h to prepare Li_2S_8 solution. A total of 20 μL of Li_2S_8 solution and 20 μL of conventional electrolyte of lithium-sulfur battery were added on the cathode side and anode side, respectively. After allowing the assembled coin cell to stand for 12 h, it was discharged at a constant current of 0.112 mA until reaching 2.06 V using the LAND CT2001A battery testing system, and then discharged at constant voltage at 2.05 V until the current dropped below 0.01 mA, generating a time-current curve.

Table S1. The fitting R_{ct} values of HEO@S, MEO@S and C@S at different temperatures.

T (°C)	R_{ct} of HEO@S (Ω)	R_{ct} of MEO@S (Ω)	R_{ct} of C@S (Ω)
30	52	85	105
40	30	55	62
50	20	29	33
60	15	19	18



The diagram shows an equivalent circuit model. It consists of a series resistor R_s on the left, followed by a parallel combination of a resistor R_{ct} and a constant phase element (CPE). The CPE is represented by a horizontal line with a right-pointing arrow underneath it. To the right of this parallel combination is a series resistor W .

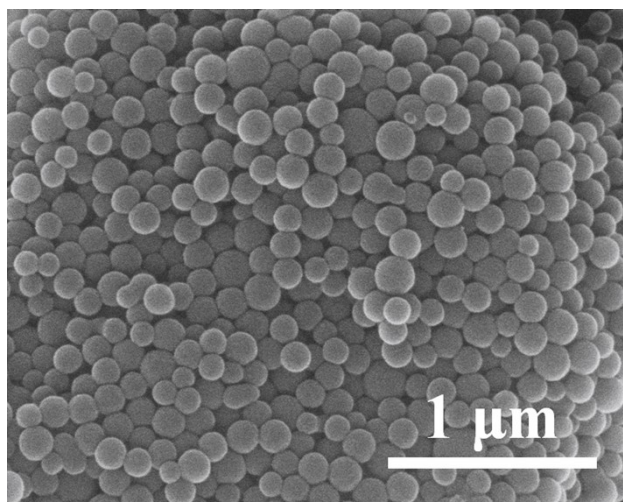


Figure S1. SEM image of carbon spheres.

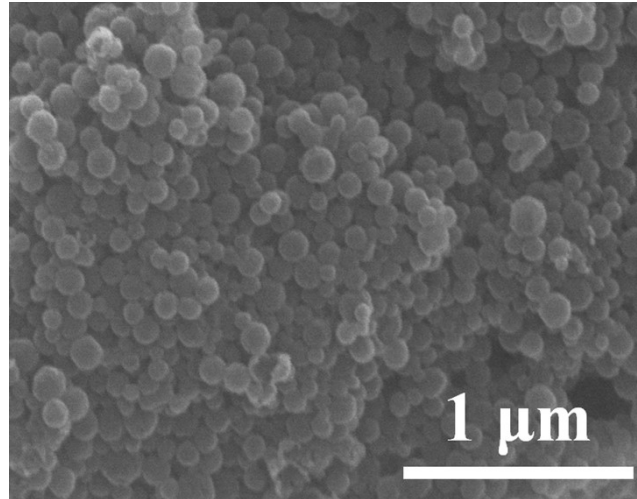


Figure S2. SEM image of HEO.

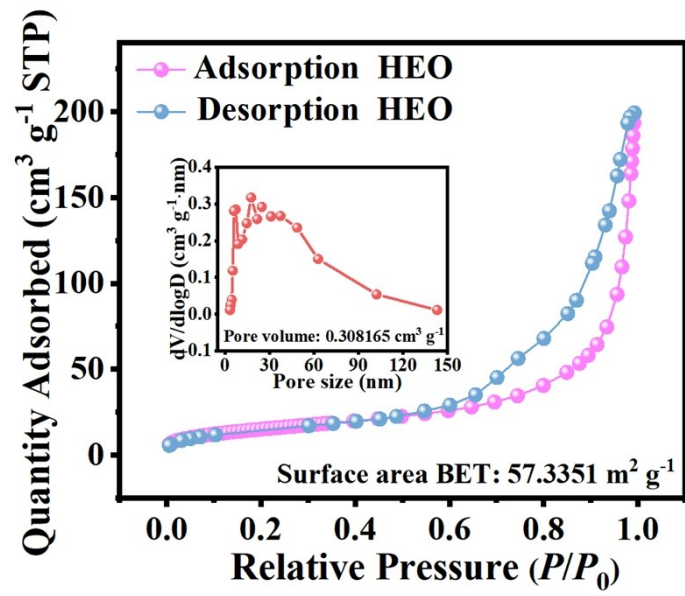


Figure S3. Adsorption-desorption isotherms and pore size distribution of HEO.

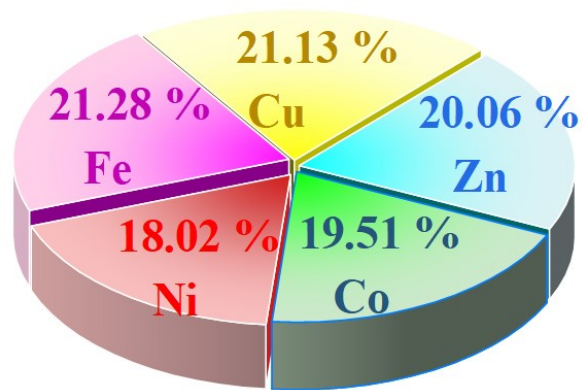


Figure S4. Element analysis of HEO with ICP-OES.

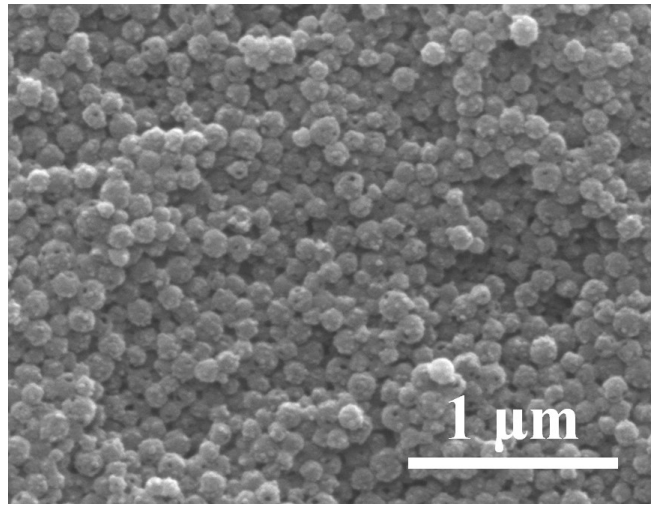


Figure S5. SEM image of HEO@S.

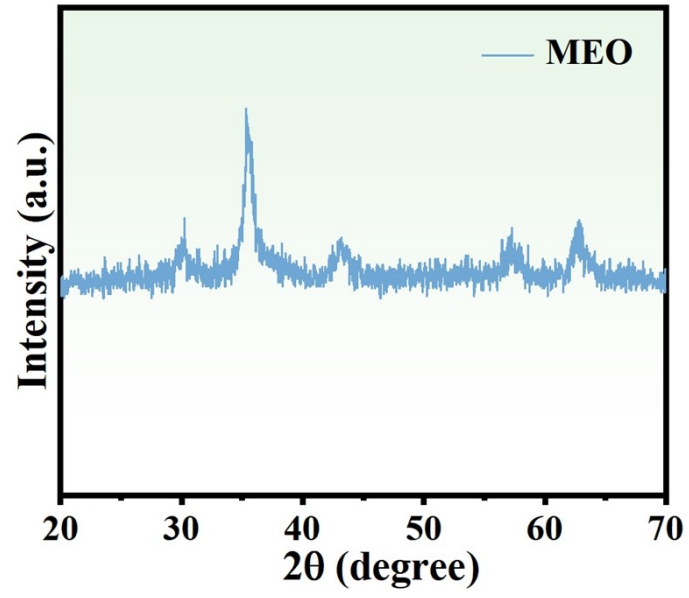


Figure S6. XRD pattern of MEO.

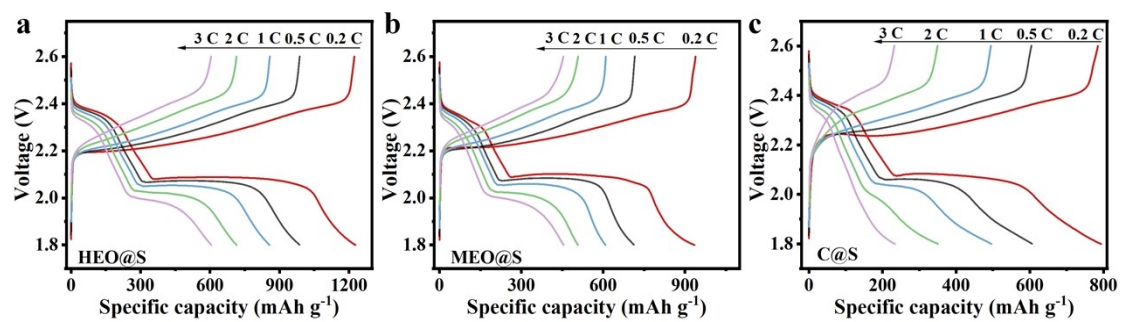


Figure S7. Galvanostatic charge-discharge (GCD) curves of (a) HEO@S, (b) MEO@S, and (c) C@S at different current densities.

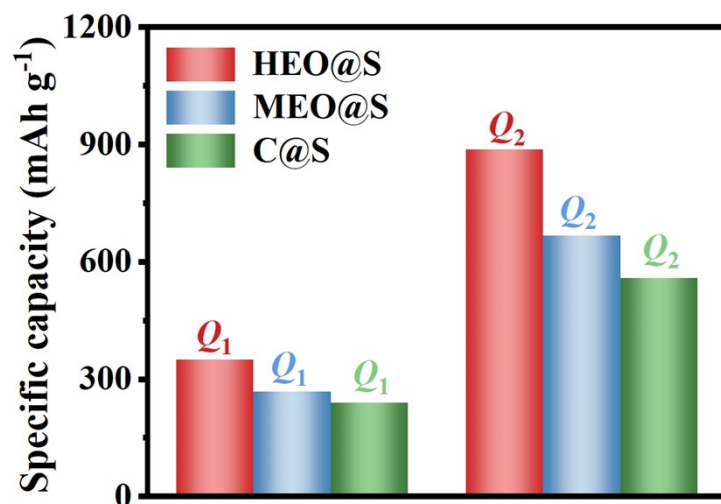


Figure S8. Histogram of the specific capacity (Q_1 and Q_2) of HEO@S, MEO@S, and C@S at 0.2 C.

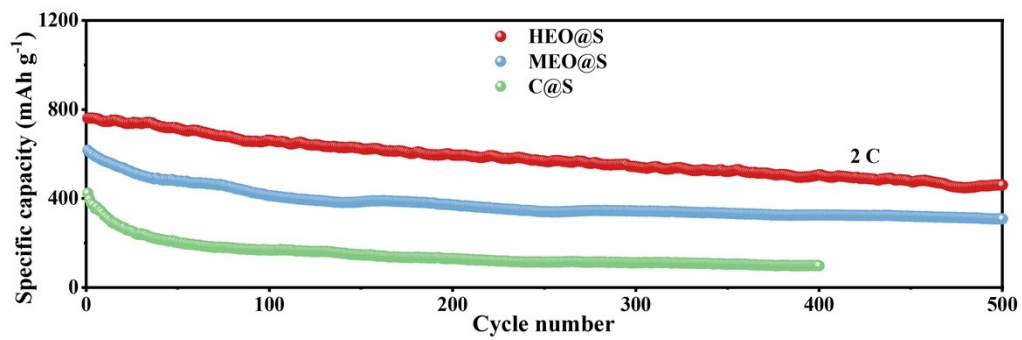


Figure S9. Long-term cycling stability of HEO@S, MEO@S, and C@S at 2 C.

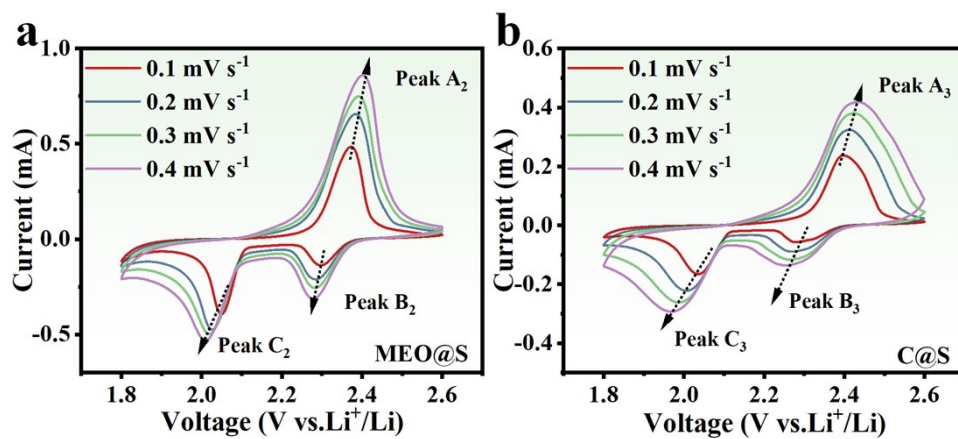


Figure S10. CV curves of (a) MEO@S and (b) C@S at scan rates of 0.1-0.4 mV s⁻¹.

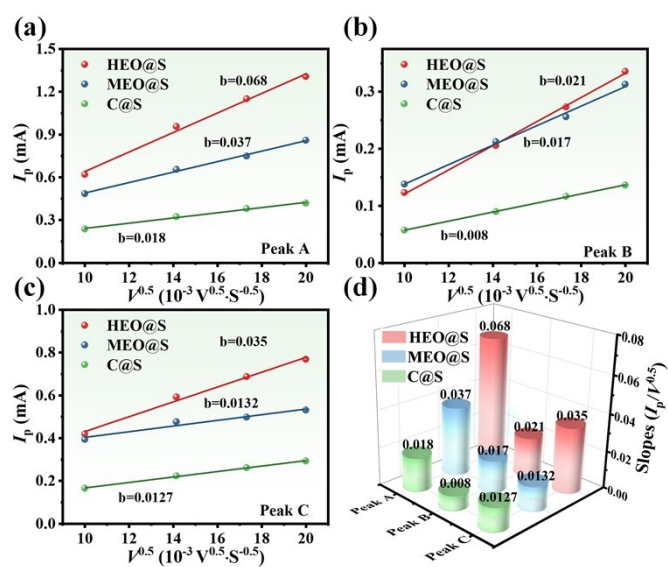


Figure S11. (a-c) Relationships between the peak currents of the oxidation/reduction peaks and the square root of the scanning rate for HEO@S, MEO@S, and C@S. (d) Values of slopes refer to lithium-ion diffusion ability of HEO@S, MEO@S, and C@S.

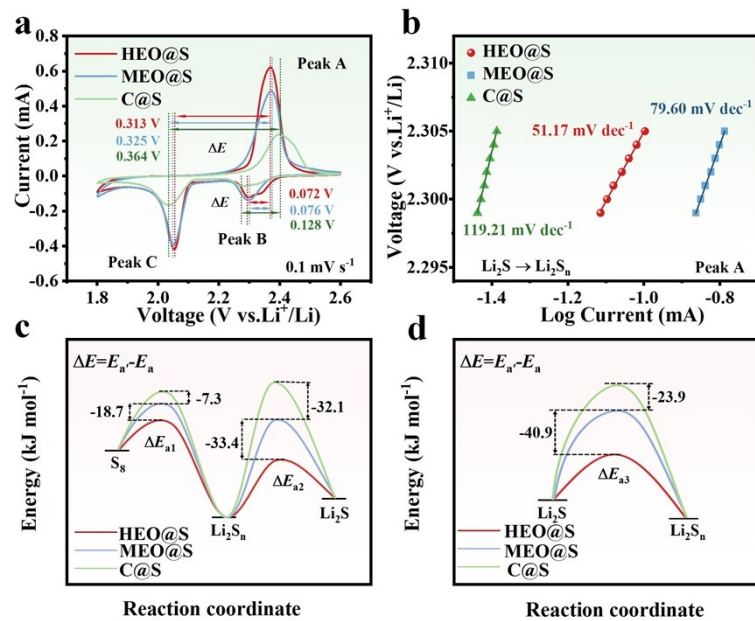


Figure S12. (a) CV curves of HEO@S, MEO@S, and C@S at 0.1 mV s⁻¹. (b) Tafel slopes of the oxidation peak based on the CV curves. Relative activation energies of (c) reduction reactions and (d) oxidation reaction.

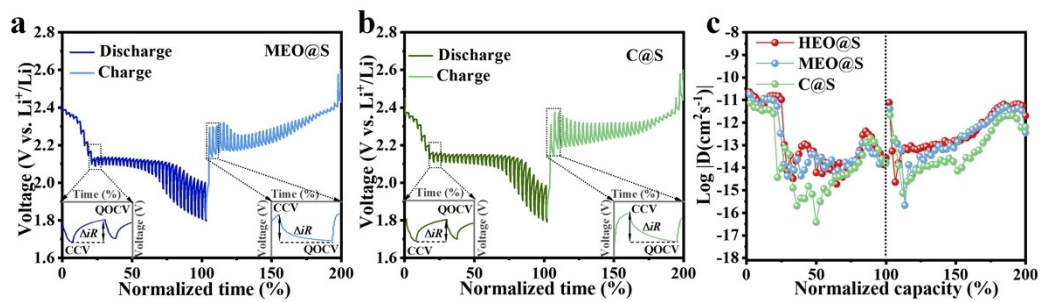


Figure S13. GITT voltage curves of (a) MEO@S and (b) C@S. (c) Calculated D_{Li^+} of HEO@S, MEO@S, and C@S.

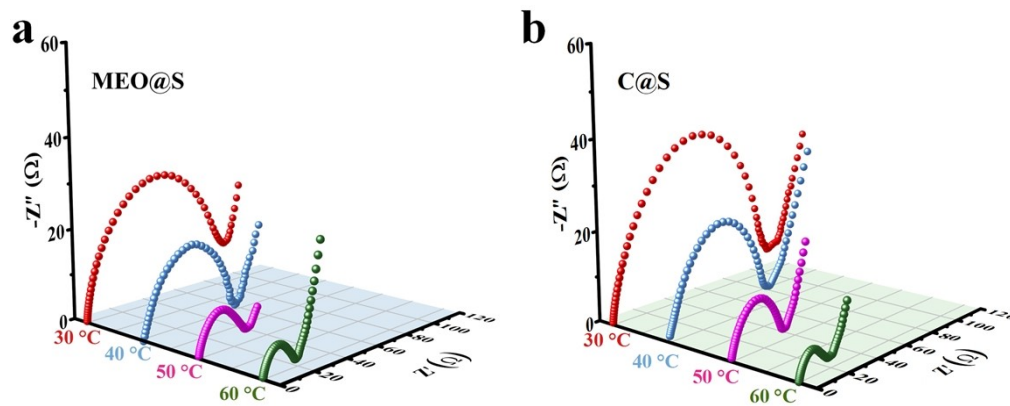


Figure S14. EIS spectra of (a) MEO@S and (b) C@S.

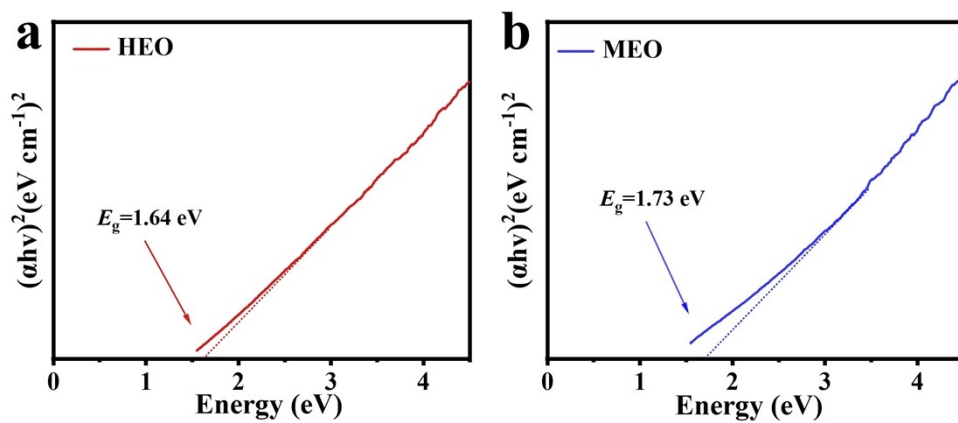


Figure S15. Tauc diagrams of (a) HEO and (b) MEO.

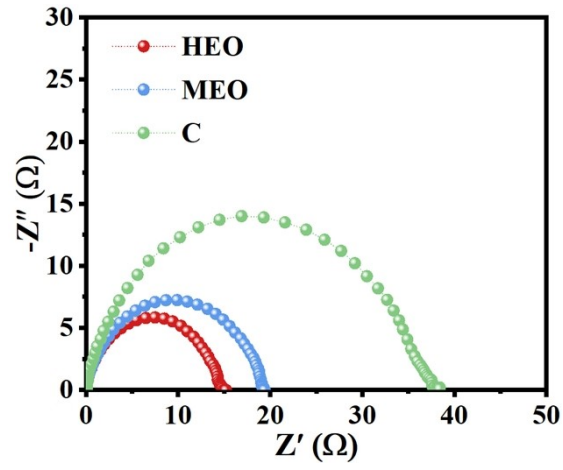


Figure S16. EIS spectra of HEO, MEO and C symmetrical batteries.

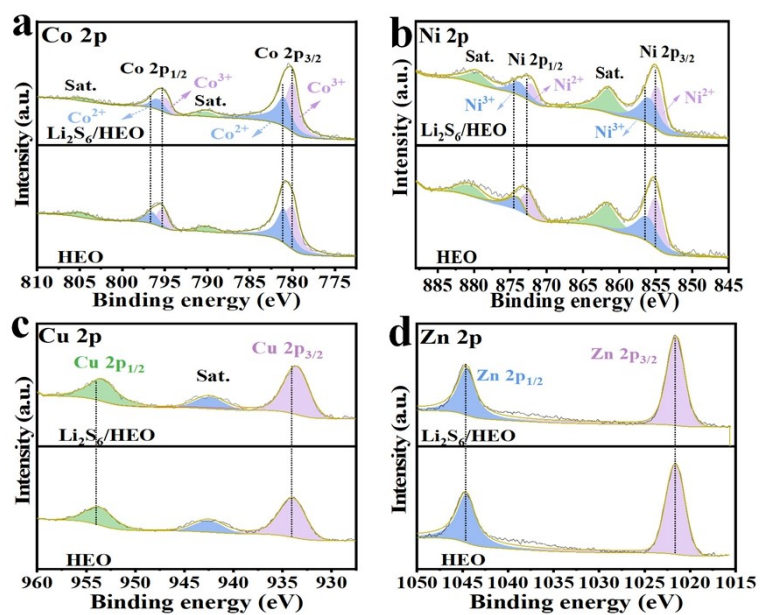


Figure S17. XPS spectra of (a) Co 2p. (b) Ni 2p. (c) Cu 2p. (d) Zn 2p of HEO before and after Li_2S_6 solution adsorption test.

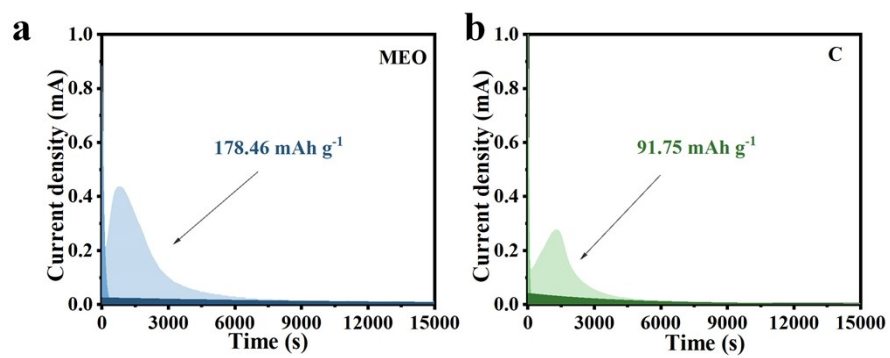


Figure S18. The deposition current versus time curves of Li_2S on (a) MEO and (b) C.